

Experimental and Numerical Investigation to Evaluate the Performance of Helical Coiled Tube Heat Exchanger

Prof. Dr. Qasim Saleh Mahdi

Lecturer. Dr. Sahar Abdul Fattah

M.Sc. student Firas juma Abd

Mech. Eng. Dept. College of Engineering, University of Al-Mustansiriyah

Abstract:

Experimental and Numerical investigation of heat transfer enhancement in shell and helical coil tube heat exchanger is carried out in the present work. Experimental work included design of helical coil heat exchanger with different curvature ratio and coil pitch. Three helical coil tube heat exchangers with different curvature ratio (D/d) 12/1, 15/1, 17/1, 20/1 and 24/1 are studied to choose the optimum one. Four helical coils with different coil pitch 1.8d, 2d, 3d, and 5d has been chosen to study the effect of coil pitch on heat transfer coefficient. From experimental results the curvature ratio 17/1 gives optimum helical coil. Experimental results show increases of coil pitch lead to increasing in heat transfer coefficient of the shell side and indicate that convective heat transfer is increased by Reynolds number as well as Dean Number.

Numerical geometry has been built using ansys fluent package 14.1 commercial copy with solid work and gambit software program depends on the optimum design . Numerical results show that the temperature decreases along the coil and the temperature difference effect on heat flow along helical coiled. Also there is different in temperature between each turn. Empirical correlation has been developed to predict Nusselt number at helical coil. The comparison between numerical and experimental results show good agreement.

Key Words: Helical ,Heat exchanger, Coiled tube.

تحقيق عملي و عددي لتقييم أداء مبادل حراري حلزوني الأنبوب

طالب ماجستير فراس جمعة

م.د. سحر عبد الفتاح عبود

أ.د. قاسم صالح مهدي

قسم الهندسة الميكانيكية / الجامعة المستنصرية

الخلاصة :

التحقيق التجريبي والعددي لتحسين انتقال الحرارة لمبادل حراري مكون من أسطوانة (القشرة) وأنبوب حلزوني نفذت في هذا العمل تضمن العمل التجريبي تصميم مبادل حراري حلزوني مع أفضل نسبة تقوس ودرجة حلزونة . خمس مبادلات حرارية حلزونية مع نسب تقوس مختلفة 1/24، 1/20، 1/17، 1/15، 1/12 درست لاختيار أفضل مبادل حراري حلزوني. أربعة مبادلات حرارية مع درجات حلزونة مختلفة (1.8d, 2d, 3d, 5d) صممت لدراسة تأثير درجة الحلزونة على معامل انتقال الحرارة. الملف الحلزوني الذي له نسبة تقوس 17/1 اختير كأفضل ملف حلزوني طبقا للنتائج العملية.

زيادة درجة الحرارة تؤدي إلى زيادة معامل انتقال الحرارة في (القشرة). النتائج العملية تشير إلى أن انتقال الحرارة يزداد بزيادة رقم رينولد بالإضافة إلى رقم ديان.

أما الجانب العددي فقد تم استخدام برنامج *ansys fluent* في رسم الشكل باستخدام برنامج *solid work* و *gambit* في التحليل وبالاعتماد على أفضل تصميم. وأظهرت الدراسة العددية أن درجات الحرارة تقل على طول الملف و الفرق درجات الحرارة له تأثير على انتقال الحرارة وهناك فرق في درجة الحرارة بين لفة وأخرى تم تطوير معادلة تجريبية لتوقع عدد ناسلت لأنبوب محلزن كما بينت المقارنة بين النتائج العملية والعددية بينت توافق جيد.

Nomenclature

List of symbol

- Ac : Cross sectional area (m²)
 As : Surface area (m²)
 Cp : specific heat (J/ kg.c°)
 D : Coil diameter (m)
 d : Tube diameter (m)
 De : Dean Number
 g :Gravity acceleration(m²/s)
 h : Heat transfer coefficient (W/m².C°)
 k : Thermal conductivity (W/m. C°)
 L : Length (m)
 \dot{m} : Mass flow rate (kg/s)
 N : Number of turn
 Nu : Nusselt number (h .d /k)
 P : Pitch (m)
 Q : heat rate (W)
 Re : Reynolds number (-)
 T : Temperature (°C)
 u : Inlet velocity to the coil side (m/s)
 V : Volume (m³).
 v: Velocity to the shell side (m/s)

Subscripts

- av : Average
 bs : Base fluid
 m : mean

Greek Letters

- μ : Dynamic viscosity (Pa.s)
 ν : Kinematic viscosity (m^2/s)
 ρ : density (kg/m^3)
 α : Thermal diffusivity (m^2/s)
 Φ :Viscous dissipation function.

Introduction:

Enhancement of the heat transfer can be achieved by employing various techniques methodologies such as increasing either heat transfer surface or increasing heat transfer coefficient between the fluid and surface that allow high heat transfer rate. In general, the enhancement technique can be divided into two types: active and passive techniques as the following:

- 1- The active techniques require external forces, e.g. electric field, acoustic, and surface vibration.
- 2- The passive techniques require special surface geometries such as roughness surface, treated surface and extended surface or fluid additives

Both techniques have been used for improving heat transfer in heat exchangers. Due to their compact structure and high heat transfer coefficient. Curved tubes have been introduced as one of the passive heat transfer enhancement techniques. Helical coil heat exchangers as shown in **Figure(1)** are common equipment found in many industrial applications running from solar energy applications, nuclear power applications, chemical and food industries and many other engineering applications.

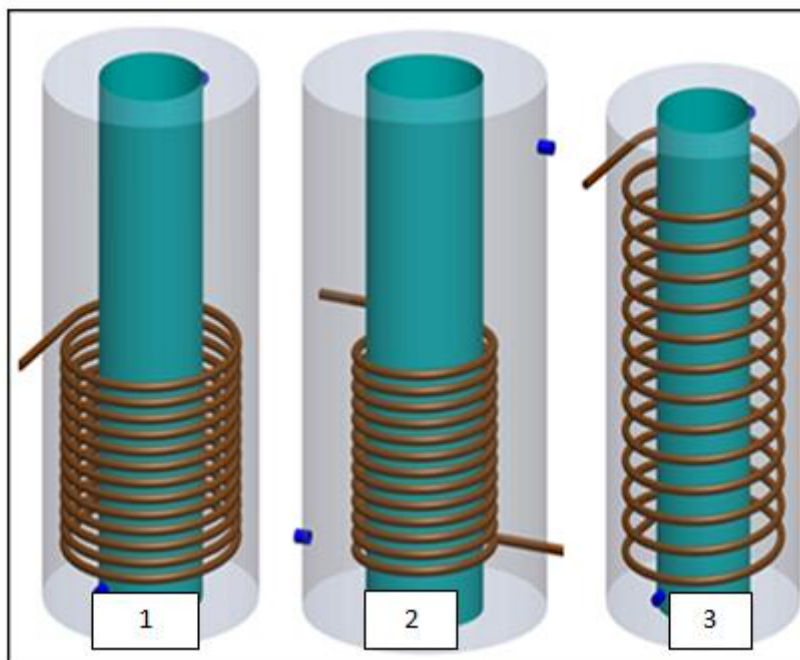


Fig .(1) Heat exchanger with different coil (1,2,3)

Heat transfer rate of helically coiled heat exchangers is significantly large because of the secondary flow pattern developed in helical coil due to the centrifugal force (**Dean Cell**) caused by the curvature of the tube **Dean**^[1]. Therefore helical coils shown in **Figure (1)** are well known types of curved tubes, which have been used in a wide variety of applications. **Drived et al.**^[2] investigated numerically the effect of secondary flow on laminar flow heat transfer in helically coiled tubes both in the fully developed region and in the thermal entrance region. The results obtained from predictions were validated with those obtained from experiments in the range in which they overlapped. **Xin and Ebadian**^[3] studied the effects of the Prandtl number and geometric parameters on the local and average convective heat transfer characteristics in helical pipes. Five helical pipes with different torsion and curvature ratios were tested with three different working fluids. The results showed that for the laminar flow region the Nusselt number changed significantly as the Prandtl and the Dean numbers increased. Based on the present data, new empirical correlations for the average fully developed were obtained. **Naphon**^[4] studied the thermal performance and pressure drop of helical coil heat exchanger with and without helical crimped fins. Cold and hot water were used as working fluids in shell and tube sides respectively, at different flow rate and different inlet temperature. The results show that for increases in mass flow rate and hot water, the cold water temperature increases. The average heat transfer rate increased when hot and cold water mass flow rates increased. It was also reported that heat exchanger effectiveness was affected by inlet hot and cold-water mass flow rates and inlet hot water temperature. **Gorgi**^[5] investigated experimentally the mixed convection heat transfer in a coil-in-shell heat exchanger for various Reynolds numbers and various dimensionless coil pitches. The experiments were conducted for both laminar and turbulent flow inside coil and the effects of coil pitch on shell-side heat transfer coefficient of the heat exchanger were studied. The particular difference in this study in comparison with the other similar studies was the boundary conditions for the helical coils. The results indicate that with the increase of coil pitch, shell-side heat transfer coefficient is increased. **Jayakumar and Mahajan**^[6] performed an experimental and CFD estimation of heat transfer in helical coiled heat exchanger. Experiments were conducted five different flow rate through the coil and at the helical pipe inlet for three different temperatures. Measurement of the flow rate (hot and cold fluid), inlet and exit temperature, the heater power input, and pump were carried out at steady-state. After validating the methodology of CFD of heat exchanger, they considering the actual fluid properties instead of a constant value is established. The experimental results are compared with the CFD calculation results using the CFD package FLUENT 6.2 and give good agreement. **Ammar**^[7] studied heat transfer coefficients of shell and helically coiled tube heat exchangers experimentally. Three heat exchangers with different coil pitches were tested for both parallel-flow and counter-flow arrangement. Water was used as working fluids in shell side and tube side. The target of this study is to investigate the performance of different shapes of helical coiled heat exchanger and to simulate the numerical work.

Theoretical model:

The main purpose of this study is concerned with the design of helical coil in different coil pitch and curvature ratios. So the basic design of helical coiled as shown in **Figure (2)** have basic assumptions as follow:

- 1- Steady- state condition.
- 2- Both fluid pass through shell and coil side pass in cross pattern and both side of heat exchanger wall with no cross or transverse mixing
- 3- No change in flow phase inside heat exchanger.
- 4- No heat generation within heat exchanger.

The simple design of helical coil heat exchanger including estimations of **Incropera and Dewitt** ^[9]:

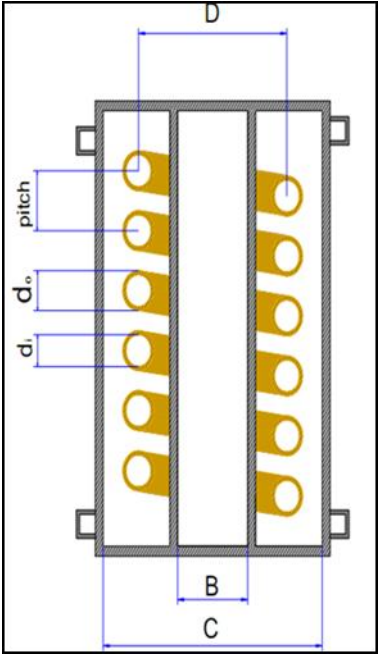


Fig .(2) Section of helical coil

heat transfer rate through helical coil (hot side)

$$Q_h = \dot{m} cp(T_i - T_o) \text{-----(1)}$$

heat transfer rate through shell side (cold side)

$$Q_{sh} = \dot{m} cp(T_i - T_o) \text{-----(2)}$$

Thermal load of heat exchanger can be calculated from:

$$Q_{av} = UA_s LMTDF \text{-----(3)}$$

The simple log mean temperature difference that is use in equation (3) can be calculated from:

$$LMTD = \frac{\Delta T_1 - \Delta T_2}{\ln \frac{\Delta T_1}{\Delta T_2}} \text{-----(4)}$$

Correction factor that are used to correct the log mean temperature difference for any deviation in this study from tube parallel of counter flow is 0.90

The thermal performance of heat exchanger was quantified by the overall heat transfer coefficient. The local heat transfer coefficient can be expressed by:

$$\frac{1}{UA} = \frac{1}{h_i A_i} + \frac{\ln \frac{d_o}{d_i}}{2pk l} + \frac{1}{h_o A_o} \text{-----(5)}$$

The average heat transfers rate can be define as:

$$Q_{av} = (Q_h + Q_c)/2 \text{-----(6)}$$

Where: Q_{av} is the average heat transfer rate between the cold portion (shell side) and hot portion (inside coil).**Pethkool** [8].

Heat Transfer Coefficient Inside the Coils

Xin and Ebadian [3] developed empirical correlations [for the average fully developed using to calculation of heat transfer coefficient inside helical coil

$$Nu = (2.135 - 0.318 De^{0.476}) Pr^{0.175} \text{----- (7)}$$

Where : $20 > De > 2000$, $0.7 > Pr > 175$

The Dean number, De , is a dimensionless group in fluid mechanics **Dean**[1], which occurs in the study of flow in curved pipes, and is defined as :

$$De = Re \left(\frac{d}{D} \right)^{0.5} \text{----- (8)}$$

In this study experimental heat transfer coefficient can be calculated from Newton's law of cooling:

$$Q_{av} = h_i A_s (T_s - T_m) \text{----- (9)}$$

Heat Transfer Coefficients Outside the Coil(Shell Side)

The heat transfer coefficient of water consists of combined effect of free and forced convection heat transfer mode according to the parameter (Gr/Re^2) . This parameter gives an indication to the dominant heat transfer Incropera and De witt ^[9].

A review of experimental data suggests a correlation of the form:

$$Nu_{comb} = \left(Nu_{forced}^n \pm Nu_{natural}^n \right)^{\frac{1}{n}} \text{----- (10)}$$

Forced Convection Heat Transfer Coefficient

In calculation the heat transfer coefficient h_o based on forced water flow, the empirical correlation due to helper was applied Incropera and Dewitt ^[9].

$$Nu_{(Df)} = CRe^m Pr^{0.333} \text{----- (11)}$$

Free Convection Heat Transfer Coefficient

The calculation of h_o for each coil can be also based on the assumption of natural convection.

$$Nu = 0.48 Ra_d^{0.25} \text{----- (12)}$$

Rayleigh number,

$$Ra = \frac{(g \beta) \rho \alpha (T_{msoc} - T_{mw}) d_o^3}{\nu \alpha} \text{----- (13)}$$

Critical Reynolds Number

Ito H. ^[10] developed the following empirical correlation to determine the critical Reynolds number

$$Re_{cr} = 2000 \left(\frac{d}{D} \right)^{0.32} \text{----- (14)}$$

Experimental Test Rig:

The schematic diagram and photo of the experimental test rig is illustrated in **Figure (3)**with the following details:

1. Heat exchanger included an external shell and internal helical coil.
2. Hot and cold water resources included; main heater, water pumps, cold water storage tank and pipes.

3. Measuring devices included ,water flow meter device with deviation error of(± 5) , Eighteen temperature thermocouples namely (T) type were calibrated with an error (± 6 %).These thermocouples have been fixed in the inlet and outlet of helical coiled and shell side and the others are fixed on the wall of helical coiled and digital control temperature.
4. Accessories included: auxiliary heater, valves, selector switch and thermometer .

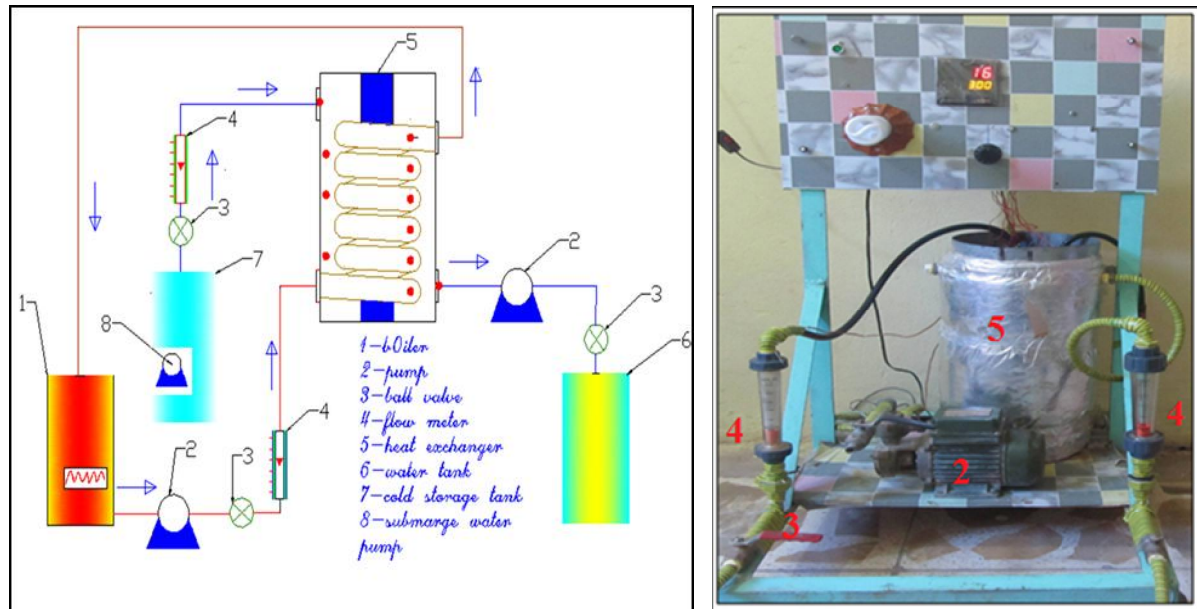


Fig .(3) Schematic Diagram and Photo Experimental Rig

Experimental procedure of present work includes many test using different shapes of helical coiled tubes (coil 1,coil 2 and coil3) as shown in **Figure (1)**. All specification of these coils are shown in **Table (1, 2)** respectively. The experimental procedure steps are:

1. Mixing ice with distilled water to supply the system by cold water.
2. Preparation of hot working fluid by using electric water heater (boiler) and then pumping to helical coil.
3. Pumping the require amount of hot and cold working fluid through the test rig and then record the flow rate. In order to control the flow rate entering to the shell and coil side a global valve are used.
4. Measuring and record the temperature along the helical coil and shell side.
5. Repeat steps (1-5) for coil 2 and coil 3.

All the tests in this study will take place after reaching the steady state condition. The tests were performing in a counter flow.

Table .(1) First group of helical coil (different curvature ratio)

Specification	Coil 1	Coil 2	Coil 3
Outer diameter of coil mm	161.5	190	228
Inner diameter of coil mm	152	180.5	218.5
Outer diameter of tube mm	9.5	9.5	9.5
Inner diameter of tube mm	7.93	7.93	7.93
No of turn	14	12	10
Pitch mm	2d	2d	2d
Length (m)	8	8	8

Table .(2) Second group of helical coil (different pitch)

Specification	Coil 4	Coil 5	Coil 6	Coil 7
Outer diameter of coil mm	161.5	161.5	161.5	161.5
Inner diameter of coil mm	152	152	152	152
Outer diameter of tube mm	9.5	9.5	9.5	9.5
Inner diameter of tube mm	7.93	7.93	7.93	7.93
No of turn	14	14	14	14
Pitch mm	1.8d	2d	3d	5d
Length (m)	8	8	8	8

Numerical Model

Numerical simulations allow the analysis of complex phenomena without resorting to an expensive prototype and difficult experimental measurements. The need for the full Navier-stokes simulation of complex fluid flows arises in numerous engineering problems. In order to analyze the flow field inside helical coil heat exchanger a solution of conservation continuity, momentum and energy equations are required. Because of complexity flow of helical coil. Thus numerical techniques have to be used to solve those equations. This part analyzes the flow inside helical coil using governing partial differential equations in three dimensions that are based on conservation of mass, momentum and energy equations.

Geometry System

The geometry system in present work consists of helical coil tube having inlet and outlet portion, cylindrical shell also have inlet and outlet portion. This system drawing by using Commercial software program called solid work premium 2012 .

Governing Equation

The conservation equation for continuity, momentum, and energy equations can be written as follows **Versteeg and Malalasekera**,^[11] with the following assumptions :

- 1- The working fluid is water and the flow characteristics are steady state.
 - 2- Newtonian fluid.
 - 3- Incompressible .
 - 4- Three dimensional .
 - 5- Laminar flow.
- Continuity Equation

$$r \left(\frac{1}{r} \frac{\partial(rv_r)}{\partial r} + \frac{1}{r} \frac{\partial(v_q)}{\partial q} + \frac{\partial v_z}{\partial z} \right) = 0 \quad \text{-----(15)}$$

-Momentum Equation in the **r** –component:

$$r \frac{\partial v_r}{\partial t} + r \left(v_r \frac{\partial v_r}{\partial r} + \frac{v_q}{r} \frac{\partial v_r}{\partial q} - \frac{v_q^2}{r} + v_z \frac{\partial v_r}{\partial z} \right) = m \left(\frac{\partial}{\partial r} \left(\frac{1}{r} \frac{\partial(rv_r)}{\partial r} \right) + \frac{1}{r^2} \frac{\partial^2 v_r}{\partial q^2} - \frac{2}{r^2} \frac{\partial v_q}{\partial q} + \frac{\partial^2 v_r}{\partial z^2} \right) - \frac{\partial P}{\partial r} + r g_r \quad \text{----- (16)}$$

-Momentum Equation in the **θ** –component:

$$r \frac{\partial v_q}{\partial t} + r \left(v_r \frac{\partial v_q}{\partial r} + \frac{v_q}{r} \frac{\partial v_q}{\partial q} + \frac{v_r v_q}{r} + v_z \frac{\partial v_q}{\partial z} \right) = m \left(\frac{\partial}{\partial r} \left(\frac{1}{r} \frac{\partial(rv_q)}{\partial r} \right) + \frac{1}{r^2} \frac{\partial^2 v_q}{\partial q^2} + \frac{2}{r^2} \frac{\partial v_r}{\partial q} + \frac{\partial^2 v_q}{\partial z^2} \right) - \frac{1}{r} \frac{\partial P}{\partial q} + r g_q \quad \text{----- (17)}$$

-Momentum Equation in the **z** –component:

$$r \frac{\partial v_z}{\partial t} + r \left(v_r \frac{\partial v_z}{\partial r} + \frac{v_q}{r} \frac{\partial v_z}{\partial q} + v_z \frac{\partial v_z}{\partial z} \right) = m \left(\frac{1}{r} \frac{\partial}{\partial r} \left(r \frac{\partial v_z}{\partial r} \right) + \frac{1}{r^2} \frac{\partial^2 v_z}{\partial q^2} + \frac{\partial^2 v_z}{\partial z^2} \right) - \frac{\partial P}{\partial z} + r g_z \quad \text{----- (18)}$$

-Energy equation :

$$r c_p \frac{\partial T}{\partial t} + r c_p \left(v_r \frac{\partial T}{\partial r} + \frac{v_q}{r} \frac{\partial T}{\partial q} + v_z \frac{\partial T}{\partial z} \right) = k \left[\left(\frac{1}{r} \frac{\partial}{\partial r} \left(r \frac{\partial T}{\partial r} \right) \right) + \frac{1}{r^2} \frac{\partial^2 T}{\partial q^2} + \frac{\partial^2 T}{\partial z^2} \right] + m f \quad \text{----- (19)}$$

Solution Method

A control-volume based technique that consists of the following steps is used for the solution of governing equations **Versteeg and Malalasekera**,^[11]:

- A grid is generated on the domain.
- For velocity, pressure, and conserved scalars, algebraic sets of equations are constructed by the integration of the governing equations on each control volume.
- Discretized equations are linearized and solved iteratively.

The pressure-based solver allows solving the flow problem in either a segregated or coupled manner. Ansys fluent provides the option to choose among five pressure-velocity coupling algorithms . For this study pressure -velocity coupling SIMPLE algorithm are used . In the present case, 1000 iterations are requested. If the residuals are still not below the proper values, then additional 500 iterations are requested as shown in **Figure (4)**. In this study a residual is 1×10^{-3} is achieved for conservation energy to avoid divergence solution, the under-relaxation is implemented as follows:

$$\Phi_{new} = (1-\alpha) \Phi_{previous} + \alpha \Phi_{calculated} \quad (20)$$

Φ_{new} : is the new under-relaxed value of Φ .

$\Phi_{previous}$: is the value of Φ from the previous iteration.

$\Phi_{calculated}$: is the calculating value.

The value for the under- relaxation factor should be in the range ($0 < \alpha \leq 1$). The values of α are 0.7 for momentum equation and 0.3 for the pressure. This is because values more than this will cause large instabilities in the solution which leads to difficult reaching convergence **Versteeg. & Malalasekera [1995]**.

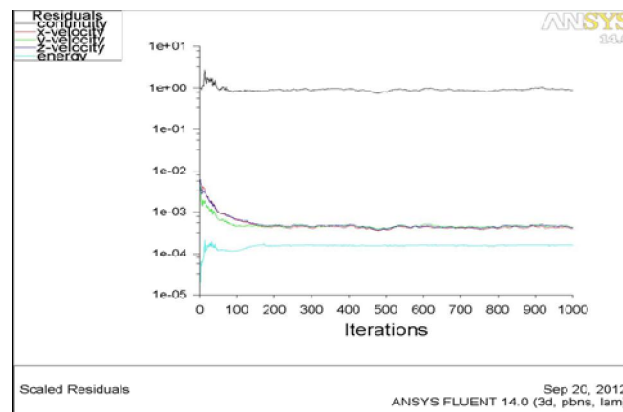


Fig .(4) Residuals for running of helical coil tube heat exchanger

Implementation of Boundary Condition:

Boundary conditions are specified for each zone of the computational domain as follow as shown in **Table (3)**:

- The velocity inlet to the helical coil is specified over a range of (0.15 to 0.5) m/sec. Constant velocity inlet to the shell side is 0.98 m/s. constant temperature inlet to the coil and shell side are (58,15)°C respectively.

- A pressure outlet is specified at the outlet domain where the pressure is assumed to be atmospheric pressure.
- No slip boundary condition is specified for the wall of coil. These conditions are used to bound fluid and solid regions.

These conditions are used to bound fluid and solid regions.

Table .(3)Boundary condition for helical coil.

Temperature inlet to coil side °C	Temperature enter to shell side °C	Velocity inlet to the coil side m/s	Velocity inlet to the shell side m/s
58	15	(0.15-0.5)	0.98

Model Validation

Figure (5) gives the validation of Nusselt numbers prediction from experimental work based on predicted Nusselt number by **Xin and Ebadian, [3]**.

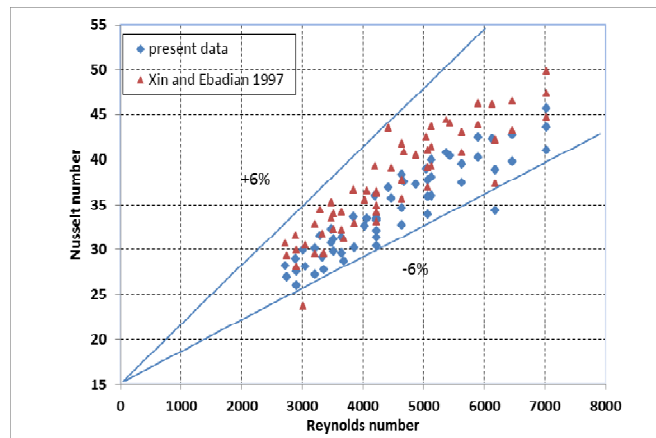


Fig .(5) validation of Nusselt numbers prediction from experimental based on predicted Nusselt by (Xin, Ebadian research 1997)

Results and Discussions

Experimental Results

Figures (6) to (8) show the temperature distribution along the turns of helical coil at different curvature ratio. From this figures it can be seen clearly the maximum gradients in temperature are appear at the first eight turn and then it became less. Also it can be seen that the best gradient of temperature appear at coil(1).

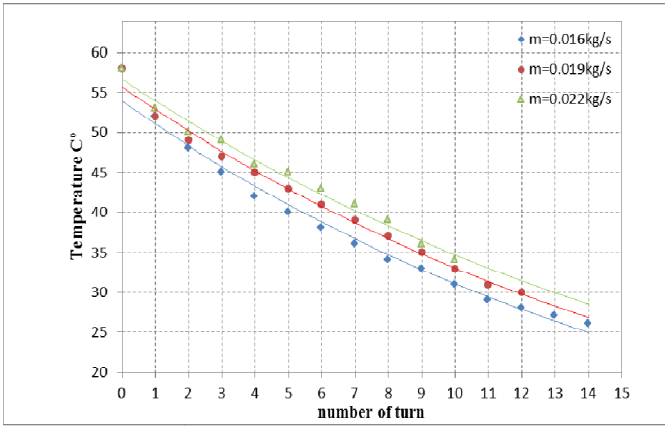


Fig .(6) Temperature distribution along helical coil (1)at different mass flow.

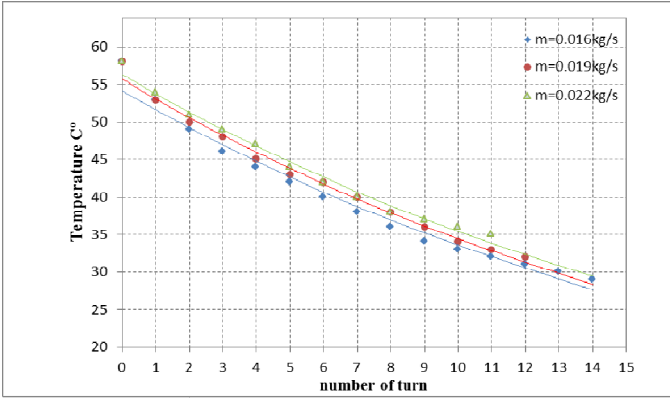


Fig .(7) Temperature distribution along helical coil (2)at different mass flow rate.

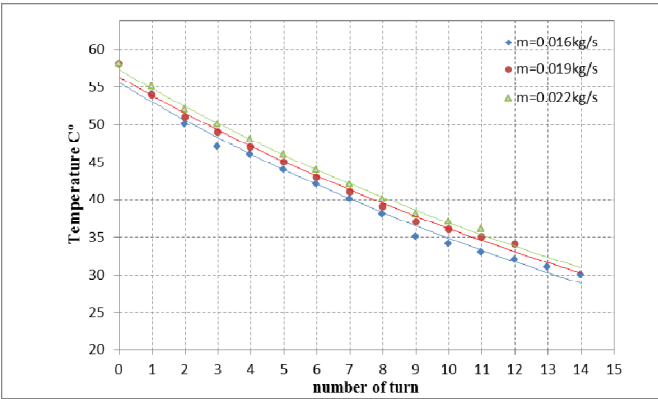


Fig .(8)Temperature distribution along helical coil (3)at different mass flow rate

Figure (9) and (10) show the effect of number of turns on Reynolds number and Nusselt number. From these figures it can be seen that the value of Reynolds number and Nusselt number decrease with increasing number of turns. Also from these figures it can be noted that the maximum heat transfers coefficient occurs at the coil(1).

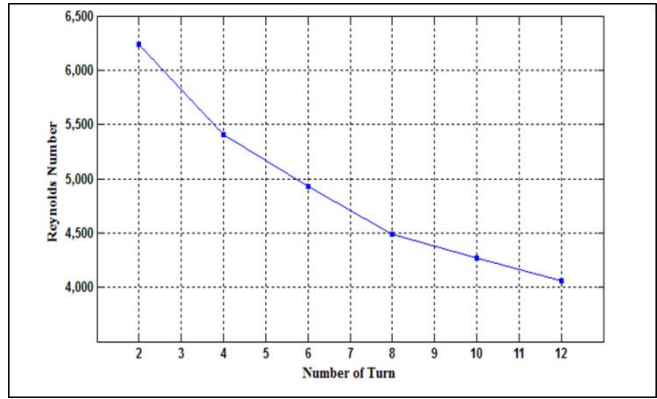


Fig .(9) Variation of Reynolds number with number of turn for helical coil (1)

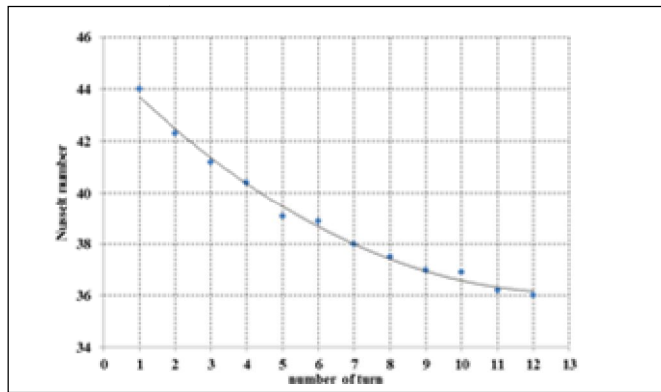


Fig .(10) Variation of Nusselt number with number of turn for coil (1)

Figures (11) shows the effect of Dean number on the value of Nusselt. Number. From this, figure increase of Dean number lead to increase Nusselt number and heat transfer coefficient because at high Dean number the vortex formation have ability to destroy thermal boundary layer and decreasing in temperature different between inner and outer surface of coil.

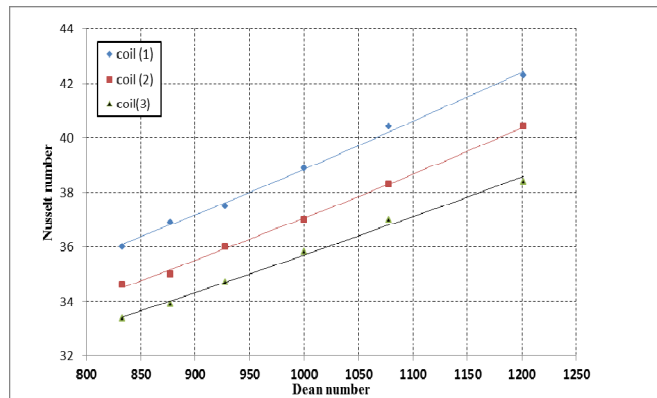


Fig .(11)) Effect of Dean number on Nusselt number for different helical coils

The effect of curvature ratio on temperature difference between inlet and outlet coil side shown in **Figure (12)** it can be seen that the maximum difference of temperature appear at the coil (1). Curvature ratios and Reynolds number have significant effect on the value of Nusselt number, Dean Number, and heat transfer coefficient. This values decrease with increasing this ratio at the same inlet condition. The maximum enhancements of heat transfer coefficient appear at the coil (1). Heat transfer coefficient of coil (1) larger than by 4%, 9% from coil (2) and coil (3) respectively. Generally heat transfer coefficient decrease with increasing curvature ratio over the optimum ratio because of the flow behavior inside helical coil with higher curvature ratio become the same behavior flow inside straight tube and flow become disable to form secondary flow that have ability to destroy the thermal boundary layer. In addition from this figures can be seen clearly from all test and results the coil(1) can be chosen an optimum coil diameter.

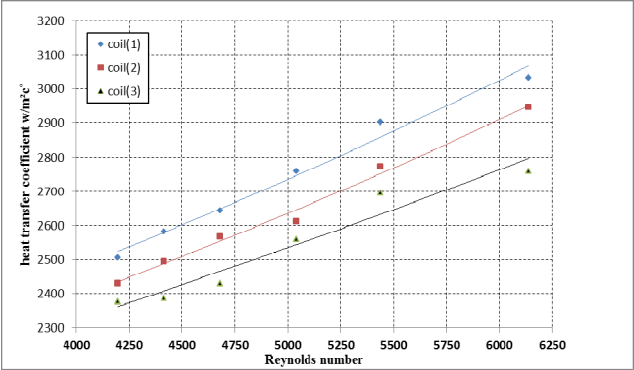


Fig .(12) Effect of curvature ratio on the Reynolds number vs. the heat transfer.

Figure (13) shows the effect of coil pitch on heat transfer coefficient in the shell side. From the results the heat transfer coefficient inside shell enhance with increase coil pitch. From this figure, it is appear that the increase of coil tube pitch lead to high value of shell side heat transfer coefficient this may be explained as follow: in smaller coil pitches, the coolant water is confined in the space between the successive coil rounds and a semi-dead zone is formed. As in this region, the flow of shell-side fluid decelerated and heat transfer coefficients will be descending.

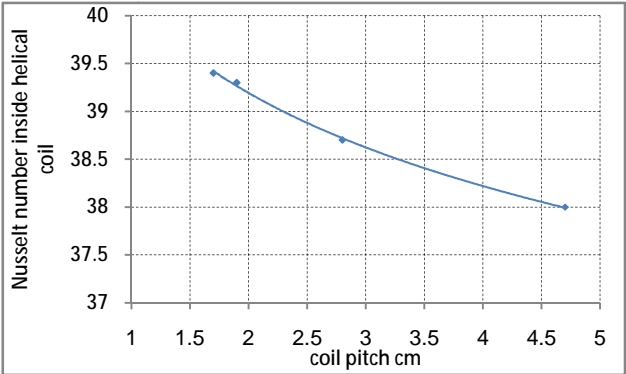


Fig .(13) Effect of coil pitch on the Nusselt number in the coil side.

Numerical Results

Heat transfer from the hot fluid flowing inside the helical tube to the cold fluid flow through the shell is analysis by using ANSYS Fluent 14. The boundary condition value that is inlet to the coil and shell side shows in **Table (3)** .**Figure (14)** to **(16)** shows temperature contours of helical coil in three dimensions at different velocity inlet and with distilled water. It can be seen gradient of temperature distribution along the helical coiled and maximum temperature occurs at center of tube

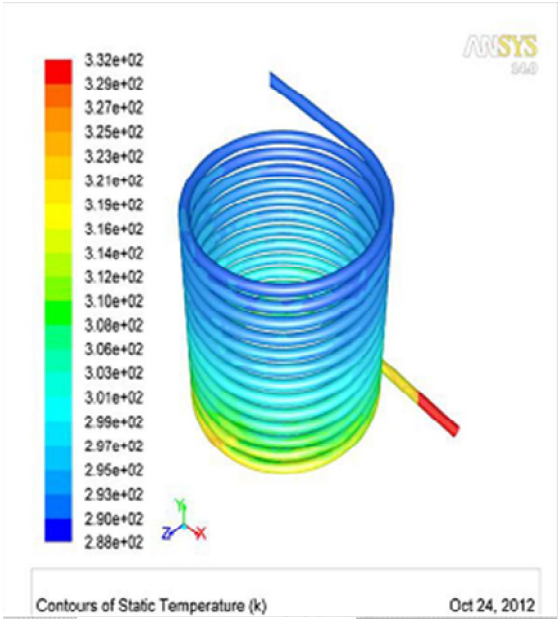


Fig .(14)Temperature contour at u=0.15m/s.

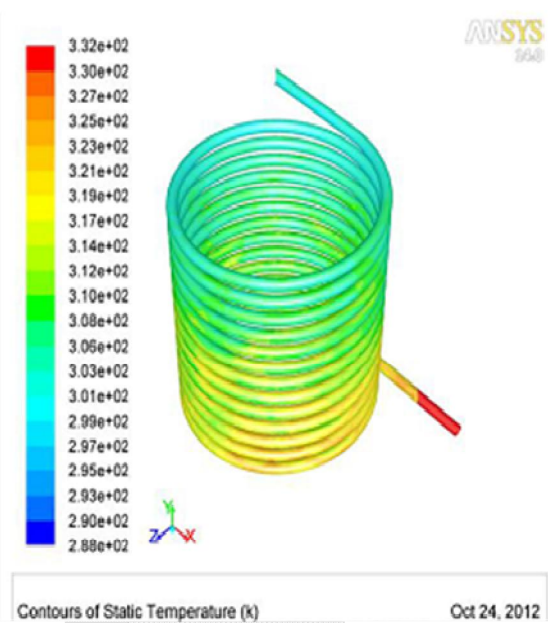


Fig .(15) Temperature contour at u=0.48m/s.

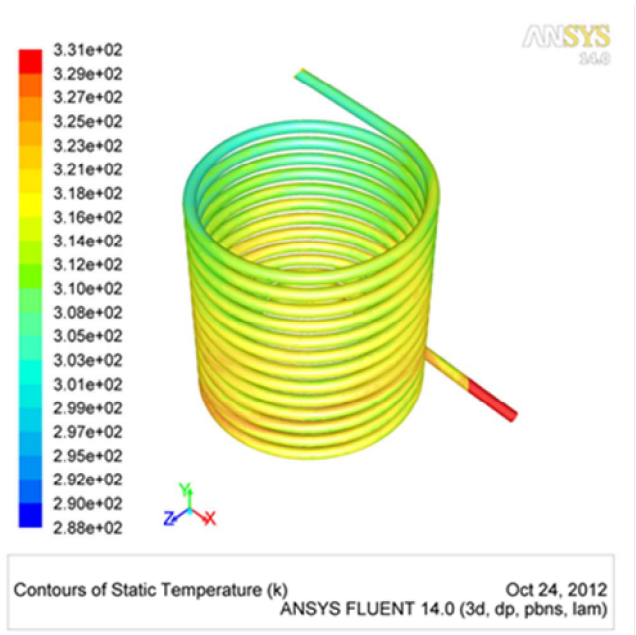


Fig .(16) Temperature contours at $u=0.5$ m/s

Figure (17) to (19) shows temperature contours at (XZ) plane section at different velocities. Figures (20) to (22) show plane section of temperature contours. From this figures it can be seen gradient of temperature distribution along the sections of turns and maximum temperature occurs at the center of tube.

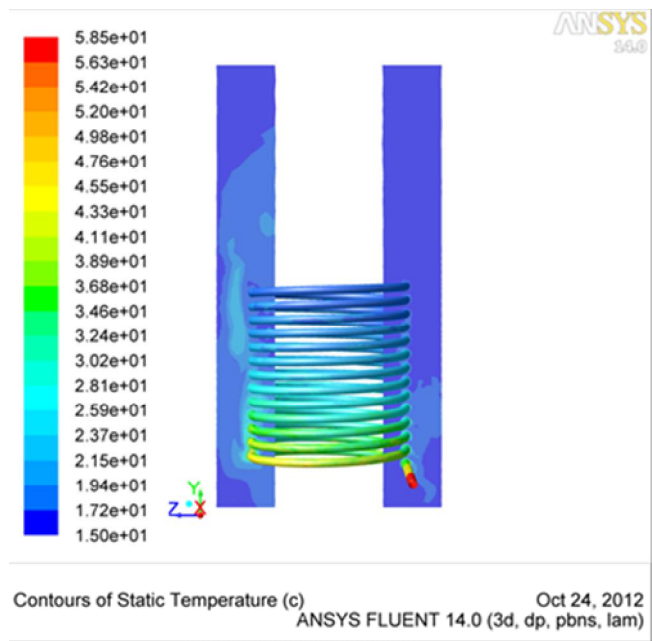


Fig .(17) Temperature counter at $u=0.15$ m/s

Fig .(18) Temperature contour at $u= 0.48\text{m/s}$

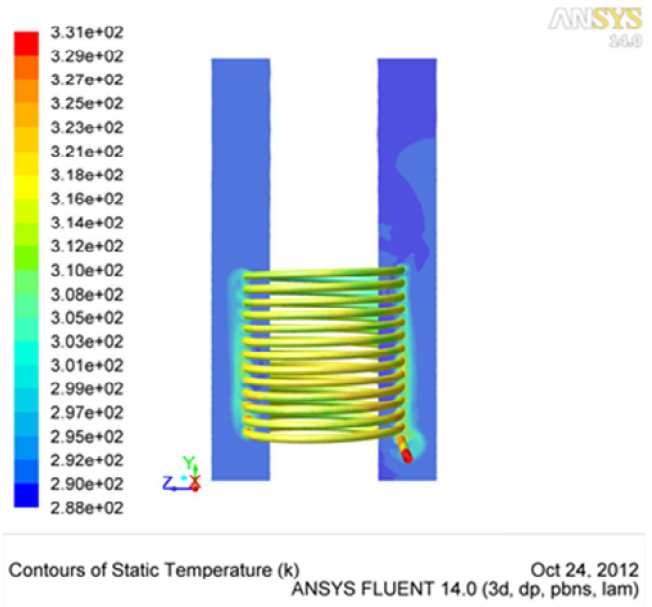


Fig .(19) Temperature contour at $u=0.5\text{m/s}$

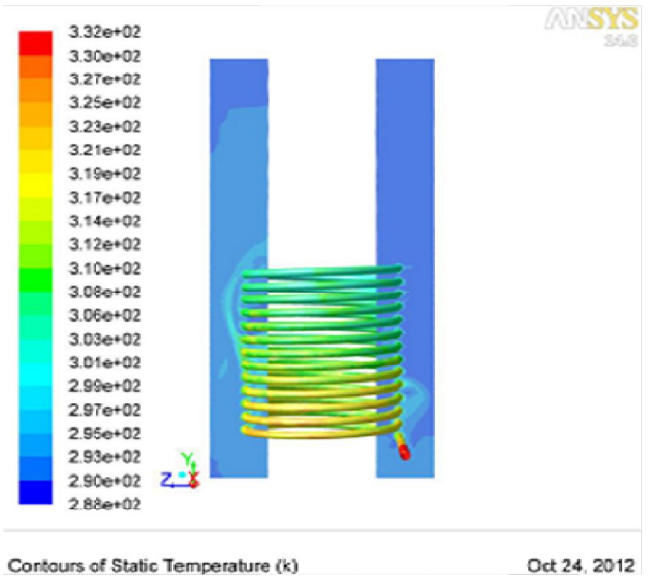
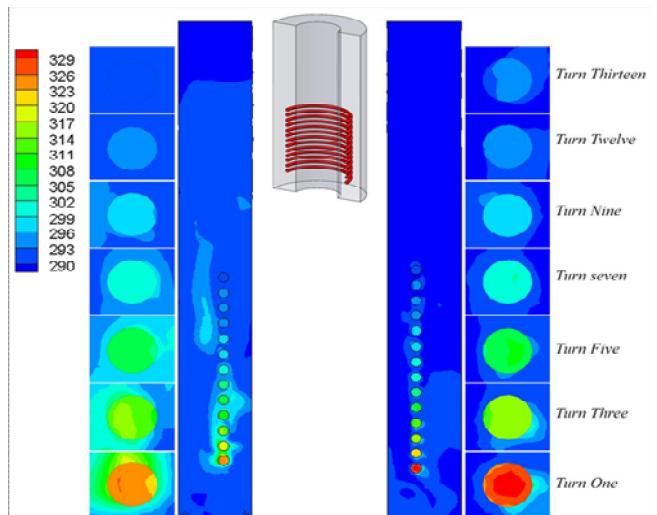


Fig .(20) Contour of temperature along turns of coil at $u=0.15\text{ m/s}$



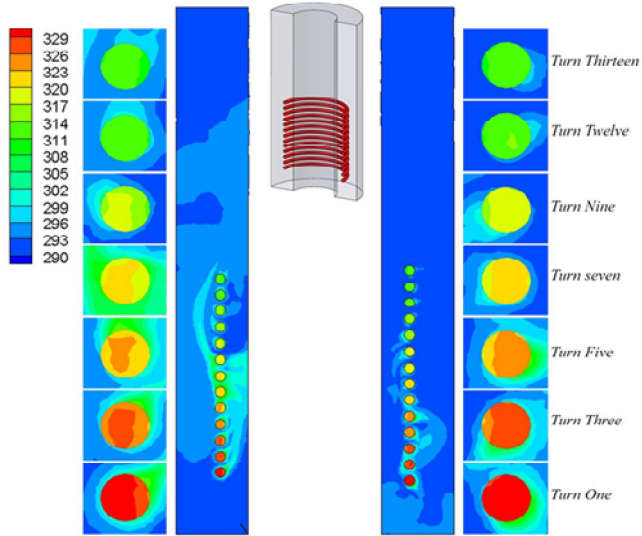


Fig .(21) Contour of temperature along turns of coil at $u=0.48\text{m/s}$

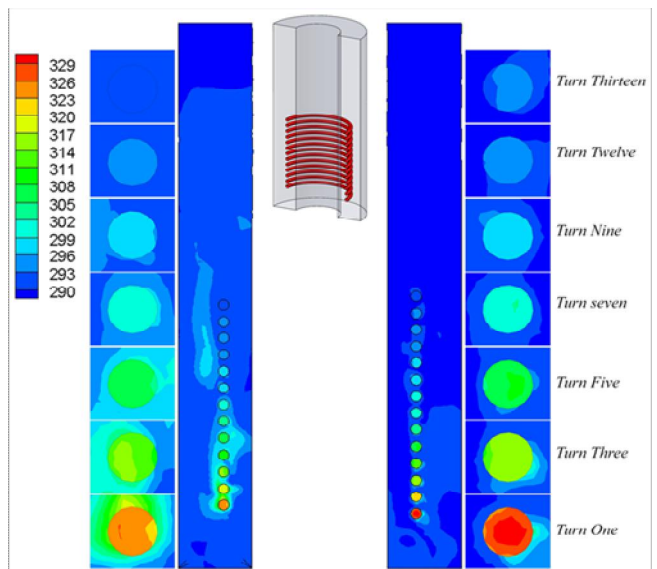


Fig .(22)Temperature contour at $u=0.5\text{m/s}$

Figures (23) to (25) shows velocity contour of helical coil along the turns. From these figures, it can be seen that, flow pattern difference along the turns. Because of secondary flow caused by centrifugal force the maximum values of velocity occur at the center of tube and then gradually decrease Dean^[1]. Velocity at inner surface of tube increasing with increases inlet velocity of tube. From these figures it can be seen that pair of counter vortex that is developing inside helical coil.

Fig .(23)Velocity contour along turn of helical coil at $u=0.15\text{m/s}$

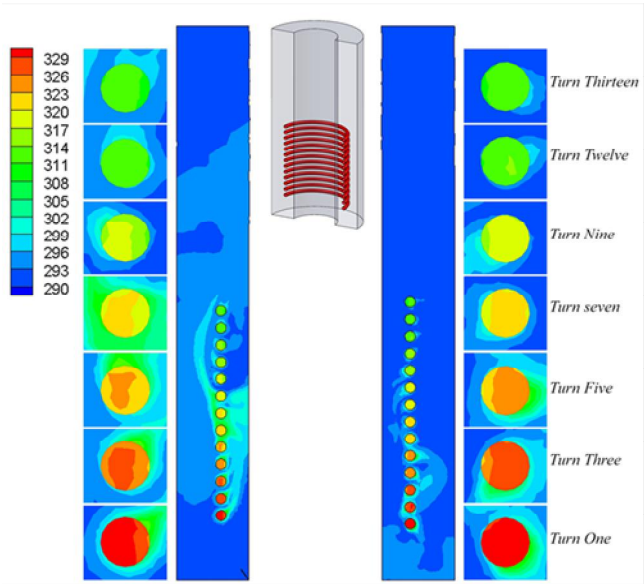


Fig .(24)Velocity contour along turn of helical coil at $u=0.48\text{m/s}$

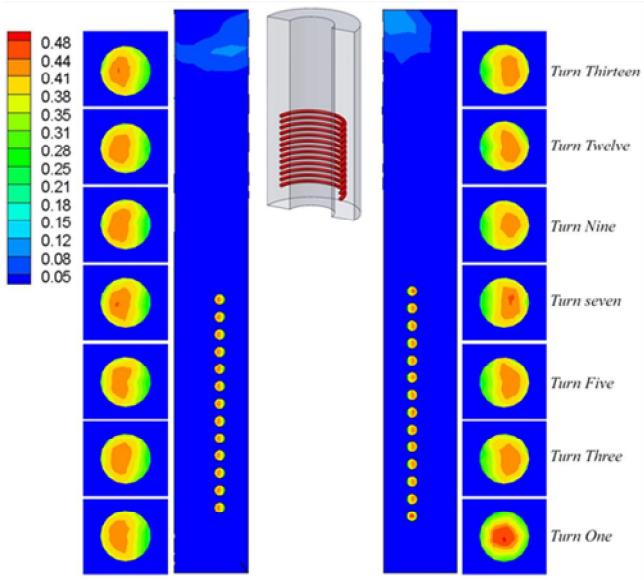
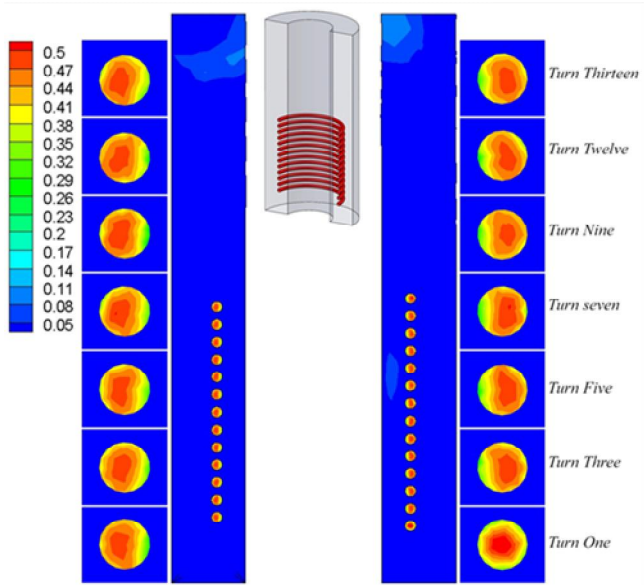


Fig .(25) Velocity contour along turn of helical coil at $u=0.5\text{m/s}$



Correlation of Nusselt Number

New empirical correlation has been developed in this study to predict of Nusselt number in the helical coil tube at laminar flow with the range of Nusselt and Prandtl number between (500 to 1500) and (3.4 to 5.5) respectively with error \pm 2% ,as compare between experimental and predict Nusselt number as shown in **Figure(26)**

$$Nu = 0.31De^{0.6323} Pr^{0.28} \quad 500 \leq De \leq 1500 \quad \text{-----(21)}$$

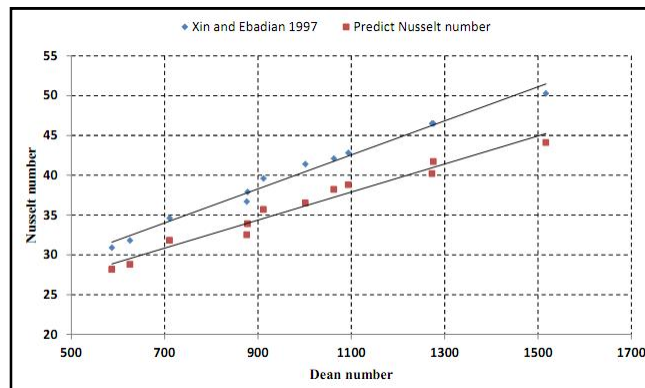


Fig .(26) Comparison between predict Nusselt number with other researcher.

References

1. Dean, W.R., " Notes on the motion of fluid in a curved pipe", Philos. Magazine ,vol(4) pp. 208–223, (1927).
2. Drived A.N, Smith K.A, Merrill E.W, Brain P.LT." Effect of secondary fluid on laminar flow heat transfer in helical coiled tube". Chemical Engineering Journal ,vol. (17). pp.1114-1122 (1971).
3. Xin R.C and Ebadian M.A, "The effect of Prandtl number on local and average heat transfer coefficient in helical pipe" . Heat transfer Journal, vol(119) pp. 463(1997).
4. Naphon, P., "Thermal performance and pressure drop of the helical-coil heat exchangers with and without helically crimped fins", International Communications in Heat and Mass Transfer, vol. 34 (3), pp. 321–330, (2007).
5. Gorgi M." experimental study of mixing convection heat transfer in vertically coiled tube" Heat exchanger experimental thermal and fluid science ,vol.(34),pp. 900-905, (2010).
6. Jayakumar, J. S. Mahajani, S. M. "Experimental and CFD estimation of heat transfer in helically coiled heat exchangers". Chem. Eng. Res. Design ,vol. (86),pp. 221-232,(2008).

7. **Ammar A. Hussain, " Experimental Study of Heat Transfer Coefficients of Shell and Helically Coiled Tube Heat Exchanger". University of Technology. Mechanical Engineering Department. M.Sc.(2011).**
8. **Pethkool .S, Eiamsa-ard S, "Turbulent heat transfer enhancement in heat exchanger using a helically corrugated tube", International Communications in Heat and Mass Transfer , vol. (38) pp.340-347(2011).**
9. **Incropera F. P. and DeWitt D. P., "Fundamentals of Heat and Mass Transfer", Fourth Edition, John Wiley & Sons, New York, (1996).**
10. **Ito H. "Friction factor for turbulent flow in curve pipe", Journal of Basic Engine, Trans. ASME, vol (81)pp.123-124, (1959).**
11. **Versteeg H. K. and Malalasekera W.," An introduction to computational fluid dynamics-The finite volume method", First Edition, Longman Group Ltd.,(1995).**